



## 저작자표시-비영리-변경금지 2.0 대한민국

이용자는 아래의 조건을 따르는 경우에 한하여 자유롭게

- 이 저작물을 복제, 배포, 전송, 전시, 공연 및 방송할 수 있습니다.

다음과 같은 조건을 따라야 합니다:



저작자표시. 귀하는 원저작자를 표시하여야 합니다.



비영리. 귀하는 이 저작물을 영리 목적으로 이용할 수 없습니다.



변경금지. 귀하는 이 저작물을 개작, 변형 또는 가공할 수 없습니다.

- 귀하는, 이 저작물의 재이용이나 배포의 경우, 이 저작물에 적용된 이용허락조건을 명확하게 나타내어야 합니다.
- 저작권자로부터 별도의 허가를 받으면 이러한 조건들은 적용되지 않습니다.

저작권법에 따른 이용자의 권리는 위의 내용에 의하여 영향을 받지 않습니다.

이것은 [이용허락규약\(Legal Code\)](#)을 이해하기 쉽게 요약한 것입니다.

[Disclaimer](#)

공학석사 학위논문

**Fabrication of adhesive hydrogel  
based on phenol-conjugated chitosan  
via high affinity enzymatic crosslinking  
for wet tissue adhesion**

습윤조직 접착을 위한 효소 가교 기반의

키토산-페놀 하이드로겔 제작

2023년 8월

서울대학교 대학원

공과대학 화학생물공학부

김 수 현

# **Fabrication of adhesive hydrogel based on phenol-conjugated chitosan via high affinity enzymatic crosslinking for wet tissue adhesion**

습윤조직 접착을 위한 효소 가교 기반의  
키토산-페놀 하이드로겔 제작

지도교수 황 석 연

이 논문을 공학석사 학위논문으로 제출함

2023년 8월

서울대학교 대학원

공과대학 화학생물공학부

김 수 현

김수현의 공학석사 학위논문을 인준함

2023년 8월

위 원 장 \_\_\_\_\_ 김 병 수 (인)

부위원장 \_\_\_\_\_ 황 석 연 (인)

위 원 \_\_\_\_\_ 한 지 속 (인)

## **Abstract**

# **Fabrication of adhesive hydrogel based on phenol-conjugated chitosan via high affinity enzymatic crosslinking for wet tissue adhesion**

**Suhyeon Kim**

**School of Chemical and Biological Engineering**

**The Graduate School of Engineering**

**Seoul National University**

For many years, there has been significant interest in adhesive substances for their capacity to serve as alternatives to sutures and staples in the closure of tissues during invasive surgical procedures. Nevertheless, the challenges related to effectively applying the adhesives in narrow spaces and achieving robust bonding in wet physiological conditions still impose substantial limitations on the practical translation of existing sealants. In this study, I propose tissue adhesive hydrogels in which three kinds of phenolic moieties, monophenol, catechol, and gallic acid are incorporated and activated via tyrosinase. Phenolic compounds serve as attractive functional groups since they can attribute to intrinsic properties of chitosan-based hydrogels such as adhesiveness, antibacterial activity, and anti-inflammation. The tyrosinase-mediated oxidation results in faster transition of phenolic moieties into reactive form than auto-oxidation. This demonstrates that phenolic group-incorporated and tyrosinase-mediated hydrogel may provide a robust and fast tissue adhesive platform for clinical applications.

**Keywords : Functional hydrogel, Adhesive, Chitosan, Phenol, Tyrosinase**

**Student Number : 2021-29435**

## Table of Contents

<b>Abstract .....</b>	<b>3</b>
<b>Table of Contents .....</b>	<b>4</b>
<b>1. Introduction .....</b>	<b>5</b>
<b>2. Materials and Methods .....</b>	<b>7</b>
2.1 Synthesis of modified chitosan	
2.2 Expression and purification of tyrosinase from <i>Streptomyces avermitilis</i> (SA-Ty)	
2.3 Quantification of quinones	
2.4 Measurement of tissue adhesive properties	
2.5 Antibacterial assay	
2.6 Radical scavenging assay	
2.7 Statistical analysis	
<b>3. Results and Discussion .....</b>	<b>11</b>
3.1 Quantitative analysis of quinones	
3.2 Adhesion test	
3.3 Antibacterial assay	
3.4 Radical scavenging assay	
3.5 Application of enzyme-mediated adhesive hydrogel : The controllable closure system for varicose veins	
<b>References</b>	
국문초록	

# 1. Introduction

Hydrogels in the field of translational medicine are sought after for the following desirable properties. First, the tissue integrative characteristic allows them to adapt to diverse surrounding environments [1]. Second, they undergo rapid transition into a functional state and fast gelation [2]. Third, they are biocompatible and possess anti-inflammatory property [3]. Particularly, the integration of biomaterials with host tissues is vital for preserving or even enhancing biofunctionalities and ensuring long-term success in medical applications. Therefore, making hydrogels to have adhesive property is an attractive strategy.

The adhesive property of hydrogel proves valuable as it enhances the diverse functionalities of hydrogel by facilitating better integration with tissues. Adhesive hydrogels have been explored for various applications, involving wound closure, tissue repair, soft robots, and as a hemostatic patch that can stop bleeding without relying on coagulants [4-6].

The ability to connect tissues plays a crucial role in general surgery, but traditional methods like sutures and staples have inherent drawbacks. Suturing involves intricate and time-consuming maneuvers, demanding considerable surgical expertise, making it less practical in emergency situations. On the other hand, surgical staplers have shown an increasing number of complications like staple malformations and misfirings. Additionally, both sutures and staples can cause mechanical damage to tissues, leading to issues such as dehiscence, leakage, and inflammation [7, 8]. Thus, tissue sealing remains a significant challenge despite recent advancements toward less invasive surgical techniques.

To address these limitations, attention has shifted towards adhesive materials as promising alternatives to sutures and staples for closing defects [9, 10]. Adhesiveness makes it possible to connect things that are apart from each other. This property let hydrogels to serve as sealants that bridge gaps generated at the surgical site during invasive surgeries. Here, I introduce a strategy for tissue sealing and repair which utilizes adhesive hydrogel to achieve rapid, robust, and conformable integration with wet tissues.

Phenolic compounds have been widely investigated as therapeutic agents for immune-suppression by relieving inflammation, antioxidant, anti-cancer effect, and regenerative ability. The proposed action mechanism of phenolic compounds is that they scavenge free radicals generated by immune cells and subsequently down-regulate tissue necrosis factors (TNFs) and interleukin-1. Among the various types of phenolic compounds, phloretic acid, hydrocaffeic acid, and gallic acid were investigated in this study.

Tyrosinase is a phenolic oxidase that has a similar reaction mechanism to that in mussel-inspired chemistry. First, tyrosinase hydroxylates phenol into catechol by adding a hydroxyl group on the ortho-position of phenol. Second, this results in the subsequent

oxidation of catechol to produce quinone under physiological condition or tyrosinase-mediated oxidative condition. Third, the reactive quinones tend to form covalent bonds with amines, thiols, or other phenolic moieties through non-enzymatic reactions such as oxidative phenol coupling, Michael addition, and Schiff-base reaction.

Tyrosinase from *Streptomyces avermitilis* (SA-Ty) was used in this study because of its unusually higher catalytic activity compared with other naturally existing tyrosinases toward phenolic moieties in mild conditions. In particular, SA-Ty has displayed significantly high enzymatic activity toward phenolic groups conjugated to long biopolymers due to their short activation pocket depth and the lack of neighboring residues that sterically hinder the enzymatic reaction. Furthermore, SA-Ty based system has substrate specificity to phenolic moieties without any side reactions.

We used chitosan as a biopolymer backbone. Chitosan is a natural polymer that participates in the oxidative reaction attributing adhesiveness. It has abundant primary amine residues so it also has inert therapeutic effect such as antimicrobial activity. Phenolic groups-incorporated chitosan is an attractive material since phenolic moieties work as versatile functional groups whose adhesive, anti-inflammation, and antimicrobial activities can be utilized in various area. Therefore, we speculated that conjugation of phenolic moieties onto chitosan and tyrosinase-mediated activation may enable the formation of rapid-adhesive hydrogel through the highly oxidative nature of phenolic moieties and tyrosinase while maintaining the bioinert effect of chitosan backbone. This work demonstrated that the oxidation of phenolic moieties via biocompatible SA-Ty enzyme would provide robust platform in the field of tissue engineering, specifically in tissue adhesive.

## 2. Materials and methods

### 2.1 Synthesis of modified chitosan

Monophenol moieties were conjugated onto the chitosan backbone using following procedures. Chitosan (2 g) was dissolved in 200ml of MES buffer (0.1M, pH4.7). Ph acid and EDC was dissolved respectively in ethanol and mixed together dropwisely by using a constant pressure pump to obtain an intermediate compound 1. Afterward, intermediate compound 2 was obtained by adding NHS (mg) dropwisely to the intermediate compound 1 solution. The intermediate compound 2 solution was incubated in ice bath under nitrogen condition. The intermediate compound 2 solution was slowly introduced into the chitosan solution followed by the dropwise addition. The mixed solution was kept in ice bath and reacted for 24h under N<sub>2</sub> condition to produce a final product, monophenol-grafted chitosan (CHI-MP). After the reaction, the CHI-MP was precipitated by introducing an excess amount of ethanol and was isolated by centrifugation and filtration. The product was kept in vacuum overnight for ethanol to evaporate until it became fully dried and was dissolved in DW (pH5). Samples were frozen at -80C in a freezer and lyophilized.

Catechol moieties were conjugated onto the chitosan backbone using following procedures. Chitosan (2 g) was dissolved in 200mL of MES buffer (0.1M, pH4.7). Hydrocaffeic acid (1 g) and DMTMM (1.480 g) were respectively dissolved in MES buffer. Then, the hydrocaffeic acid solution and DMTMM solution were mixed dropwisely by using a constant pressure drop funnel. The mixed solution was added to the chitosan solution dropwisely by using the same method. This mixture was kept for 12h under nitrogen protection at room temperature. After the reaction, the catechol-conjugated chitosan was precipitated by introducing an excess amount of ethanol and was isolated by centrifugation and filtration. The product was kept in vacuum overnight for ethanol to evaporate until it became fully dried and was dissolved in DW (pH5). Samples were frozen at -80C in a freezer and lyophilized.

Gallic acid moieties were conjugated onto the chitosan backbone using following procedures. Chitosan (2000mg) was dissolved in 200ml of MES buffer (0.1M, pH4.7). Gallic acid (3734mg) and EDC (3404mg) was dissolved respectively in ethanol and mixed together dropwisely by using a constant pressure pump to obtain an intermediate compound 1. Afterward, intermediate compound 2 was obtained by adding NHS (2524mg) dropwisely to the intermediate compound 1 solution. The intermediate compound 2 solution was incubated in ice bath under nitrogen condition. The intermediate compound 2 solution was slowly introduced into the chitosan solution followed by the dropwise addition. The mixed solution



was kept in ice bath and reacted for 24h under N<sub>2</sub> condition to produce a final product, gallic acid-grafted chitosan (CHI-GA). After the reaction, the CHI-GA was precipitated by introducing an excess amount of ethanol and was isolated by centrifugation and filtration. The product was kept in vacuum overnight for ethanol to evaporate until it became fully dried and was dissolved in DW (pH5). Samples were frozen at -80C in a freezer and lyophilized.

## **2.2 Expression and purification of tyrosinase from *Streptomyces avermitilis* (SA-Ty)**

Recombinant plasmids producing tyrosinase were constructed in a previous study [11, 12]. The 6mL of cultured cells was transferred into a flask with 400mL of fresh LB and 400uL of Ampicillin. The flask was further incubated at 37 C and 200 rpm. Then, 20ul of 1M IPTG and 200ul of 1M CuSO<sub>4</sub> were added for inducing cells to produce tyrosinase. The flask was incubated at 18 C and 200 rpm for 20h for the enzyme production. The cultured solution was centrifuged at 6000 rpm for 10 min, while maintaining the solution always at 4 C. The supernatant was discarded and the remaining cell pellets were washed with 50mM Tris-HCl buffer at pH 8 twice. The cells were lysated by ultra-sonication with a cell pellet released in 5mL of 50mM Tris-HCl buffer. The lysated solution was centrifuged at 15000 rpm for 30 min at 4C. The soluble fraction of crude cell soup was collected and incubated with Ni-NTA agarose bead for general His-tag purification. The tyrosinase was purified by the polyhistidine sequence contained in the expressed enzymes.

## **2.3 Quantification of quinones**

The quantitative analysis of quinones was conducted by measuring the absorbance of adducts of quinones and 3-methyl-2-benzothiazolinone hydrazine (MBTH) at 505nm with UV-spectroscopy (TECAN infinite m200 pro, Switzerland). Each material and MBTH were dissolved in deionized water at a concentration of 10mg/ml. In the 50ul of each sample, 50ul of SA\_Ty solution was added to the tyrosinase-treated group and the same volume of 50mM Tris-HCl buffer was added instead to the untreated group. The, 50ul of MBTH solution was introduced into each well of 96 well plate. The UV absorbance at 505nm was recorded right after the introduction of MBTH solution.

## **2.4 Measurement of tissue adhesive properties**

To assess the adhesion performance of the hydrogels, we employed two distinct mechanical testing methods. We measured the shear strength by lap-shear tests and the tensile strength by tensile tests, both conducted in accordance with specific testing

standards. For evaluating adhesion performance, we selected wet porcine skin as the model tissue due to its mechanical robustness and resemblance to human skin [13].

In order to measure shear strength, we employed the standard lap-shear test specified by ASTM F2255 with a Universal Testing Machine (UTM, 100 N of load cell, EZ-SX STD, Shimadzu, Japan). The samples used in the test were prepared with an adhesion area measuring 2.5 cm in width and 1 cm in length. A constant probe speed of 5 mm per minute was maintained throughout the testing process to ensure consistent and reliable measurements. The shear strength was determined by dividing the maximum force applied by the UTM by the adhesion area of the samples.

In order to measure tensile strength, we employed the standard tensile test specified by ASTM F2258 with a Universal Testing Machine (UTM, 100 N of load cell, EZ-SX STD, Shimadzu, Japan). The samples used in the test were prepared with an adhesion area measuring 2.5 cm in width and 2.5 cm in length. A constant probe speed of 5 mm per minute was maintained throughout the testing process to ensure consistent and reliable measurements. The tensile strength was determined by dividing the maximum force applied by the UTM by the adhesion area of the samples.

## **2.5 Antibacterial assay**

Antimicrobial activity of each material was evaluated using minimum inhibitory concentration (MIC) following previously reported method with certain modifications [14]. Chitosan, CHI-MP, CHI-CAT, and CHI-GA were respectively dissolved in 50mM acetate buffer (pH5). Subsequently, the resulting solutions were added to each well of a 96-well plate to result in the final concentration of 0.1, 0.2, 0.4, 0.8, 1.6, and 3.2 mg/ml. Additional acetate buffer was added in order to adjust the total volume of acetate buffer in every well to 50ul. *Staphylococcus aureus* was used for gram-positive bacteria and *Escherichia coli* was used for gram-negative bacteria. Each bacterial suspension in LB broth was added to each well to reach initial concentration of  $10^8$  CFU/ml. Additional LB was added in order to adjust the total volume of each well to 200ul. A well without any material was used as a negative control (N). Triplicate samples were performed for each test material and concentration. After incubation (37 °C, 24 h), the growth of each bacteria was measured by reading absorbance at 600nm using microplate reader (TECAN infinite m200 pro, Switzerland). MIC was determined as the lowest concentration of each material at which the bacterial growth rate was close to 0.

## **2.6 Radical scavenging assay**

In this study, a radical scavenging assay was performed to evaluate the antioxidant activity of three chitosan-based hydrogels: CHI-MP, CHI-CAT, and CHI-GA. The 10mg of each hydrogel was prepared and soaked in 1ml of distilled water for 24 hours. A 0.25 mM solution of 2,2-diphenyl-1-picrylhydrazyl (DPPH) (Sigma Aldrich, USA) was prepared in methanol. To conduct the assay, 100  $\mu$ L of the hydrogel solution was mixed with 100  $\mu$ L of the DPPH solution in each well of a 96-well plate. Triplicate samples were performed for each test material. The  $\alpha$ -tocopherol was used as a positive control. All samples were incubated in a light-protected atmosphere for 15 minute. After the reaction, the absorbance of the resulting solution was measured at 517 nm using a spectrophotometer.

## **2.7 Statistical analysis**

All data were expressed as mean  $\pm$  standard deviation (SD). Statistical analysis of the parametric data was performed using a one-way analysis of variance (ANOVA) with Tukey multiple comparisons tests. All plotting of data and statistical analyses were performed using GraphPad Prism 8.1 (GraphPad Software, La Jolla, CA, USA). (ns, not significant; \* $p < 0.05$ ; \*\* $p < 0.01$ ; \*\*\* $p < 0.001$ ; \*\*\*\* $p < 0.0001$ )

## **3. Results and Discussion**

### **3.1 Quantitative analysis of quinones**

To evaluate the formation of quinone adduct, we conducted the 3-methyl-2-benzothiazolinone hydrazine (MBTH) assay. Quinones are generated as the phenolic moieties are oxidized and MBTH can form a covalent bond with quinones. The adduct of quinone-MBTH can be quantified by measuring absorbance at 505 nm. We observed formation of the adduct over time until the graph reaches plateau (Fig. 3A). We confirmed that all three chitosan variants produced more quinones and transformed faster when tyrosinase was introduced. This indicates that tyrosinase facilitates fast and quantitative oxidative reaction. Among the tyrosinase-treated groups, CHI-MP showed greater quinone formation than other two groups. The initial oxidation rate (the slope at zero point of each graph in Fig. 3A) was shown in Fig. 3B. The final amount of oxidated adducts were compared by analyzing the graphs in Fig. 3A at 120 min at which the graphs reach plateau. This shows that CHI-MP was oxidized fast and quantitatively when it comes to the both results at initial zero point and the time the graphs reach plateau.

### **3.2 Adhesion test**

To investigate the adhesion strength of hydrogels, two mechanical tests were conducted to measure both shear strength and tensile strength. When it comes to tissue adhesion, both hydrogel and tissue possess a net negative charge under physiological conditions, leading to repulsion and hindering adhesion. However, in this study, a promising solution was explored by introducing phenolic compounds onto chitosan hydrogel, enabling the creation of tissue adhesive properties regardless of net charge. This adhesive hydrogel can compensate the drawbacks of commercial products (i.e., cyanoacrylate glue and fibrin

glue). These commercial sealants exhibit weaknesses when used in wet conditions due to low adhesion. Additionally, they solidify into rigid polymers that lack stretchability and are stiffer than the adhered soft native tissues, causing an adhesive-host compliance mismatch, functional failure, and delayed tissue regeneration. Overcoming these limitations, the hydrogel-based bioadhesive has strong advantage. Upon contact between the dry bioadhesive interface and a wet tissue surface, the hydrogel undergoes hydration, effectively drawing water from the tissue surface, forming robust integration with the tissue surface. Once adhered to the tissue surface, the bioadhesive transforms into a thin layer of chitosan hydrogel with high water content, softness, and stretchability. These mechanical properties closely match those of soft biological tissues, enhancing compatibility and promoting optimal functionality. In addition, phenolic moieties in the hydrogel can form multiple covalent bonds with tissues, which were accelerated especially with the assistance of tyrosinase. Therefore, we can expect fast and robust adhesive platform which synergistically accommodates these functionalities.

### **3.3 Antibacterial assay**

The MICs of CHI, CHI-MP, CHI-CAT, CHI-GA were determined to quantitatively evaluate their antibacterial activity. Concentrations that change by two-fold degree were tested with each material and the concentration that decreased bacterial growth significantly ( $p < 0.05$ ) compared to the 2-fold diluted concentration was determined as MIC (Fig. 5A). This result indicated that CHI-CAT and CHI-GA strongly inhibited both Gram-positive and Gram-negative bacteria as long as CHI. Many charged groups in CHI derivatives make them more water-soluble and increase the ability of interacting with bacterias, taking a chance to result in death of bacterial cells. In roughly pH 6 medium, the microbial membrane is negatively charged and the functional groups on each material are positively charged so the surface of bacteria can interact with the materials.

### **3.4 Radical scavenging assay**

To examine the radical scavenging properties, DPPH, a stable free radical species was introduced into the hydrogel solution. When DPPH reacts with radical scavenger, the rate of radical scavenging can be measured by the colorimetric change of DPPH at 517 nm of absorbance. The  $\alpha$ -tocopherol, vitamin E, was used as a positive control. As the number of hydroxyl groups in phenolic moiety increases, the radical scavenging ability of hydrogel was elevated. The radical scavenging ability of phenolic compounds demonstrates that hydrogels

can become more biocompatible by mitigating the level of inflammation they cause.

### **3.5 Application of enzyme-mediated adhesive hydrogel : The controllable closure system for varicose veins**

I anticipate developing the enzyme-mediated adhesive hydrogel as a new platform for the treatment of varicose veins if SA-Ty is replaced with PaTy (photoactivatable tyrosinase) [15]. Varicose veins are enlarged and twisted veins, typically found in the lower extremities. The exact cause is not fully understood but involves genetic factors, weakened vein walls, faulty valves, and increased pressure within the veins.

Conventional treatments for varicose veins involve surgically removing the problematic veins (stripping). Since lengthy blood vessels are pulled out of the body in this method, it is likely that physical damage and post-operative pain occur. On the other hand, other alternative approaches involve ablation of the vessels by using heat energy generated by high-frequency (RFA) or laser (ELVA). Since high temperature is applied, there is a risk of inadvertently damaging surrounding nontarget healthy tissues. Additionally, patients may still need to endure inconvenience of wearing compression stockings for a while even after surgery.

When it comes to CAVA, as soon as cyanoacrylate is injected into the blood vessels, polymerization and closure begin by many negatively charged molecules located in the inner wall of vessels which act as nucleophiles. The downside of CAVA is that adhesion starts as soon as the material enters. Therefore, medical operators need to beware of violating regulations that is injecting a certain amount of material in a certain interval of vessel when performing surgery. They sometimes even use a metronome to give a strict discipline to the movement of their hands during operation.

Changing the mechanism by which adhesiveness is expressed can design a better platform for reaching the controllable closure system. Improving controllability by incorporating external-stimuli-triggered adhesion would be a great advantage, because it is possible to reduce the inconvenience of conforming to the procedure at regular intervals and regular amounts while even measuring seconds. I anticipate reaching this goal by replacing the reaction mechanism to enzyme-mediated system. The use of PaTy instead of SA-Ty may enable the light-triggered controllable closure system by the following process. The light radiation converts PaTy into active form as the the o-nitrobenzyl tyrosine (ONBY) which blocks the active site is photo-cleaved and removed from the active site resulting in the recovery of tyrosinase activity. Until a stimulation of PaTy, the injected material can remain in a mobile phase having potential for transition into desired location and topology in the blood vessel.

This makes surgeons easily re-organize and manipulate the surgical site even after a while after the injection.

## References

1. Lee, B.P. and S. Konst, *Novel hydrogel actuator inspired by reversible mussel adhesive protein chemistry*. Advanced Materials, 2014. **26**(21): p. 3415-3419.
2. Hou, S., et al., *Rapid self-integrating, injectable hydrogel for tissue complex regeneration*. Advanced healthcare materials, 2015. **4**(10): p. 1491.
3. Singh, A. and N.A. Peppas, *Hydrogels and scaffolds for immunomodulation*. Advanced materials, 2014. **26**(38): p. 6530-6541.
4. Liu, X., et al., *Recent advances on designs and applications of hydrogel adhesives*. Advanced Materials Interfaces, 2022. **9**(2): p. 2101038.
5. Lang, N., et al., *A blood-resistant surgical glue for minimally invasive repair of vessels and heart defects*. Science translational medicine, 2014. **6**(218): p. 218ra6-218ra6.
6. Yuk, H., et al., *Rapid and coagulation-independent haemostatic sealing by a paste inspired by barnacle glue*. Nat Biomed Eng, 2021. **5**(10): p. 1131-1142.
7. Annabi, N., et al., *Elastic sealants for surgical applications*. European journal of pharmaceutics and biopharmaceutics, 2015. **95**: p. 27-39.
8. Taboada, G.M., et al., *Overcoming the translational barriers of tissue adhesives*. Nature Reviews Materials, 2020. **5**(4): p. 310-329.
9. Reece, T.B., T.S. Maxey, and I.L. Kron, *A prospectus on tissue adhesives*. The American journal of surgery, 2001. **182**(2): p. S40-S44.
10. Kjaergard, H.K., *Suture support: is it advantageous?* The American journal of surgery, 2001. **182**(2): p. S15-S20.
11. Lee, S.H., et al., *Using tyrosinase as a monophenol monooxygenase: A combined strategy for effective inhibition of melanin formation*. Biotechnol Bioeng, 2016. **113**(4): p. 735-43.
12. Kim, S.H., et al., *Tissue adhesive, rapid forming, and sprayable ECM hydrogel via recombinant tyrosinase crosslinking*. Biomaterials, 2018. **178**: p. 401-412.
13. Li, J., et al., *Tough adhesives for diverse wet surfaces*. Science, 2017. **357**(6349): p. 378-381.
14. Li, K., et al., *Antibacterial activity and mechanism of a laccase-catalyzed chitosan-gallic acid derivative against Escherichia coli and Staphylococcus aureus*. Food Control, 2019. **96**: p. 234-243.
15. Lee, U.J., et al., *Light-Triggered In Situ Biosynthesis of Artificial Melanin for Skin Protection*. Adv Sci (Weinh), 2022. **9**(7): p. e2103503.



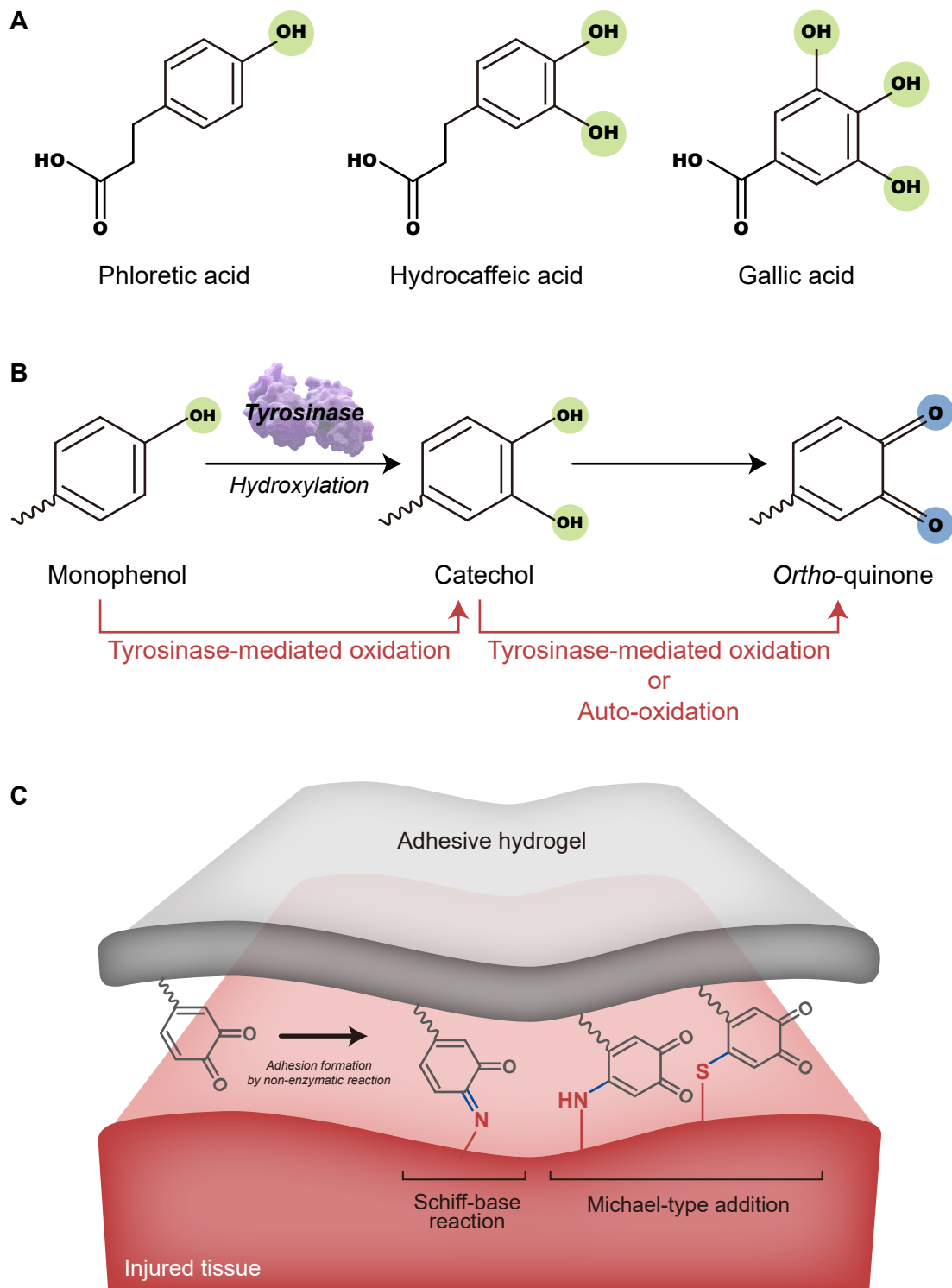


**Figure 1. (A)** Chemical structures of three phenolic compounds used in fabricating adhesive hydrogel ; Phloretic acid, Hydrocaffeic acid, Gallic acid. **(B)** The change in chemical structure of phenolic group when oxidation progresses through tyrosinase-mediated reaction or auto-oxidation. **(C)** Adhesion formation by generating covalent bonds between hydrogel and tissue via non-enzymatic reaction (i.e., Schiff-base reaction and Michael-type addition)

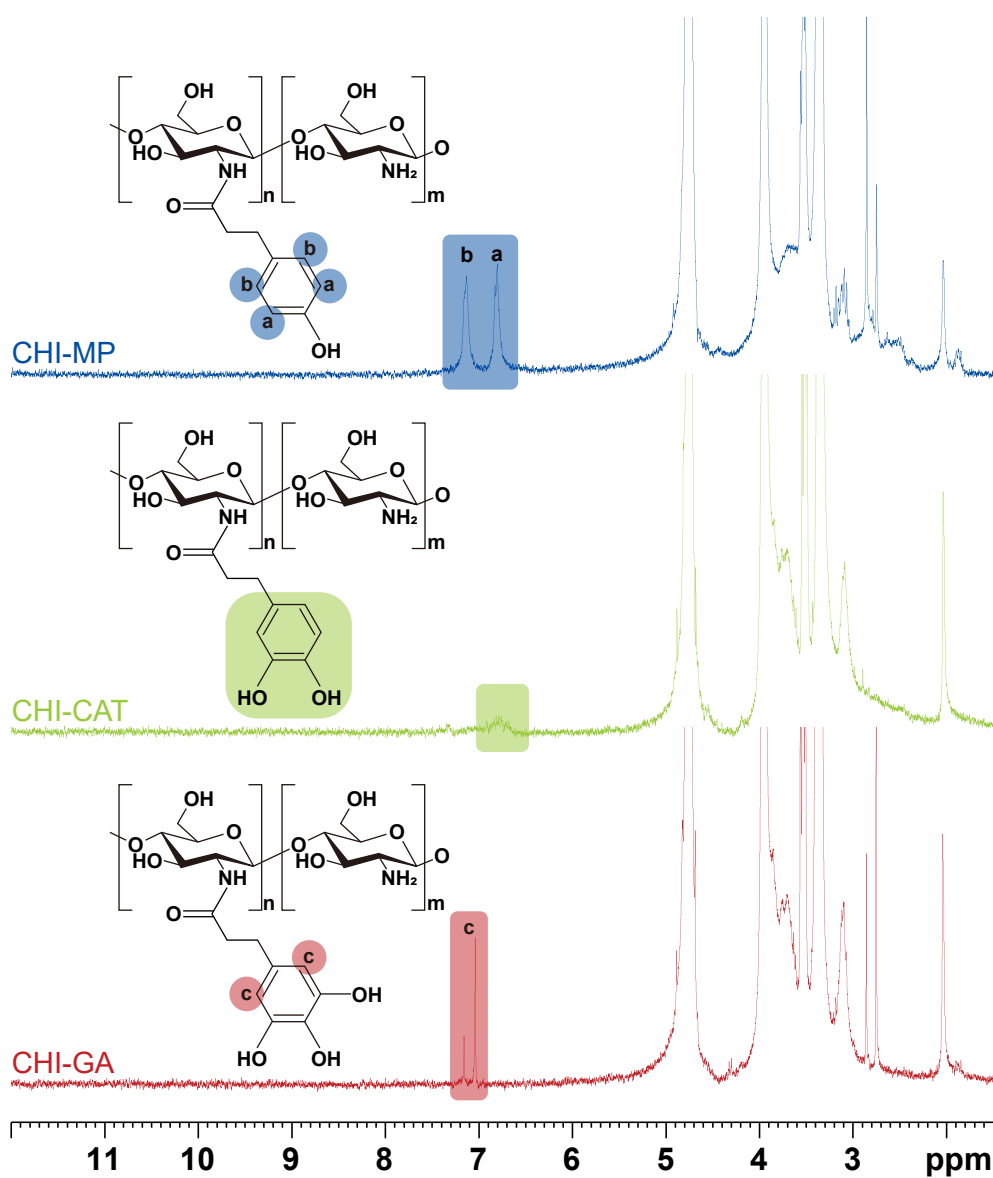


**Figure 2**  $^1\text{H}$ -NMR spectra of CHI-MP, CHI-CAT, and CHI-GA (300Hz, in  $\text{D}_2\text{O}$ )

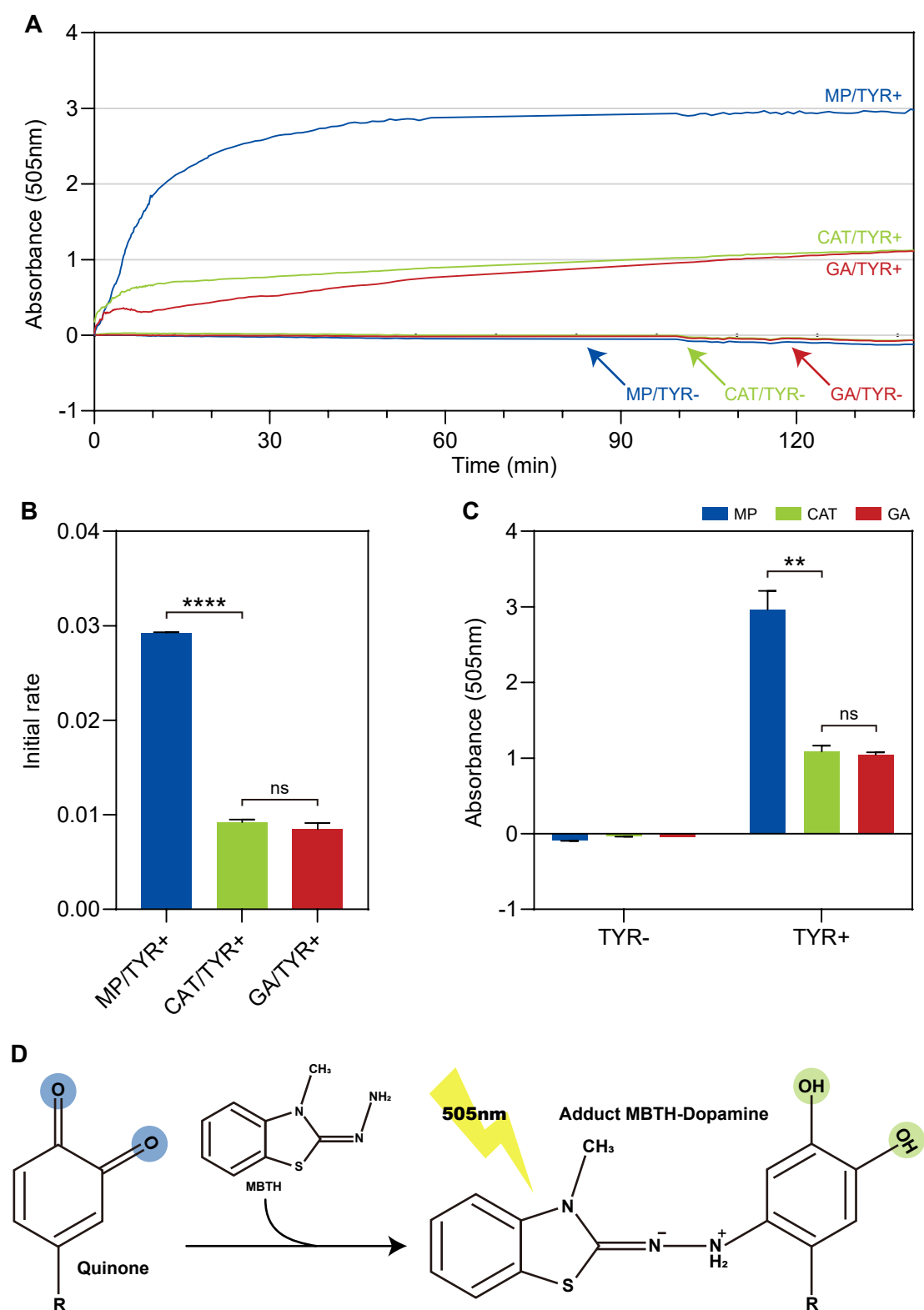


**Figure 4. Quantitative analysis of oxidation by measuring the amount of quinone.** (A) The phenolic oxidation of CHI-MP, CHI-CAT, and CHI-GA were quantified, both in the presence and absence of tyrosinase by measuring the adduct of MBTH assay at 505 nm over time until 140 min. (B) The initial oxidation rates of each phenolic moiety in tyrosinase-treated group by analyzing the slopes of Figure 4A at the zero points. (C) The final oxidated amounts of phenolic moieties at were compared by analyzing the absorbance at 120 min where the graphs of Figure 4A reach plateau. (D) Scheme of the proposed reaction mechanism of MBTH assay. The oxidated form of phenolic moieties, o-quinone, reacts with MBTH to produce MBTH-dopamine adduct.

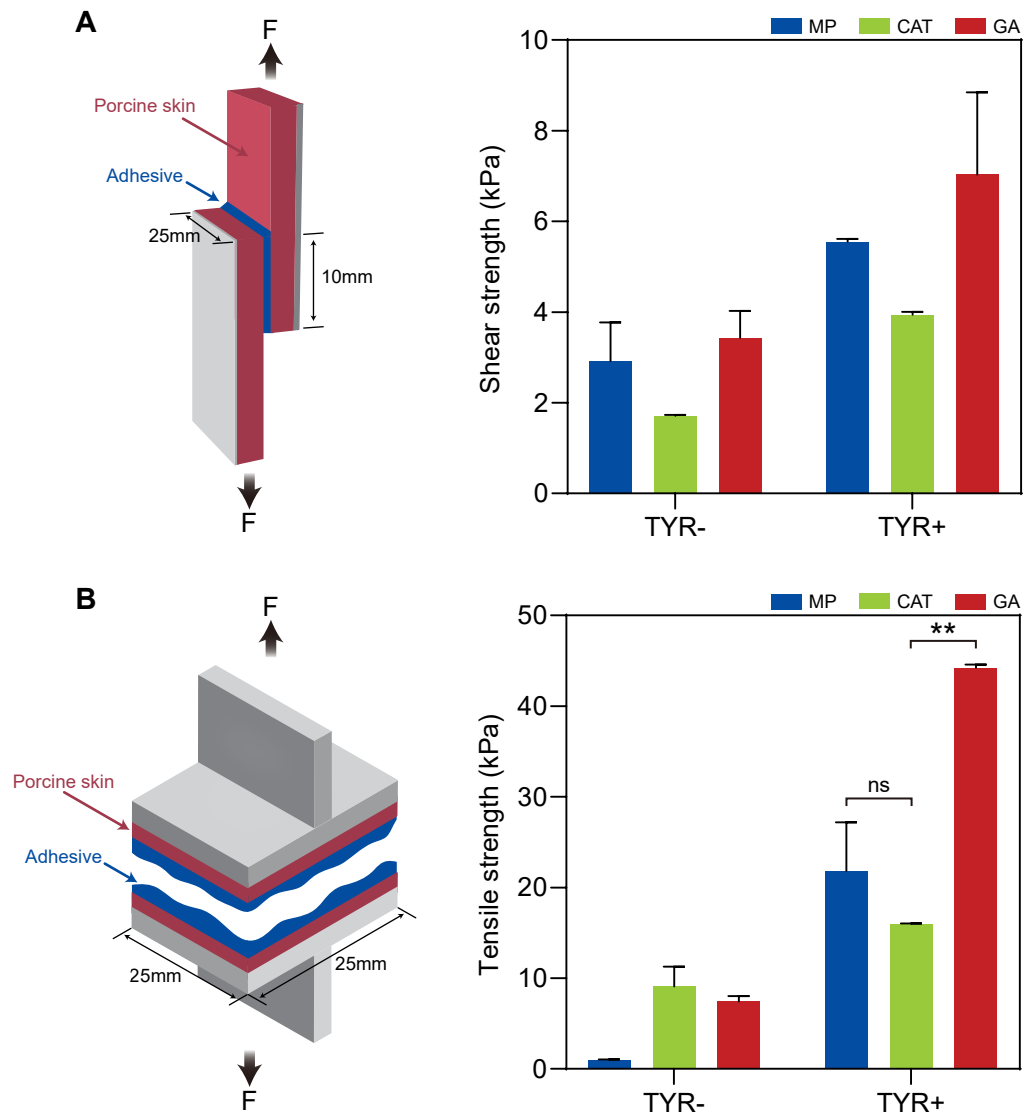


**Figure 5. Adhesion performance of hydrogels integrated to wet tissues. (A)** Setup for measurement of shear strength, based on the standard lap-shear test (ASTM F2255) and the resulting graph. **(B)** Setup for measurement of tensile strength, based on the standard tensile test (ASTM F2258) and the resulting graph.

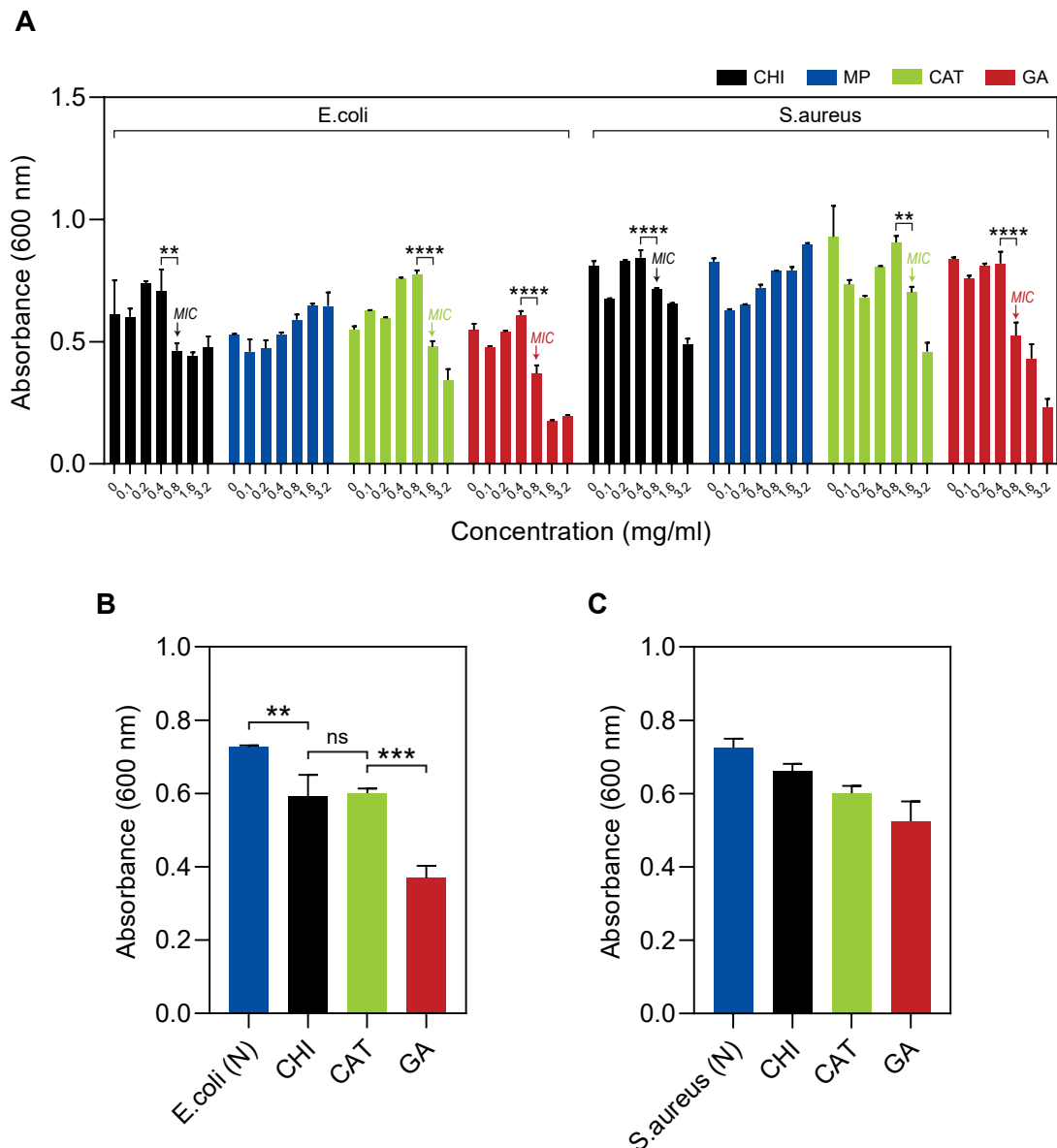


**Figure 6. Antibacterial assay.** (A) Minimum inhibitory concentrations (MICs) of CHI, CHI-MP, CHI-CAT, and CHI-GA against *E. coli* and *S. aureus* were determined. (B) The microbial inhibitory effect of CHI, CHI-CAT, and CHI-GA at the concentration of their own 1xMIC through measuring the growth of *E. coli* after 24 hours. (C) The microbial inhibitory effect of CHI, CHI-CAT, and CHI-GA at the concentration of their own 1xMIC through measuring the growth of *S. aureus* after 24 hours.

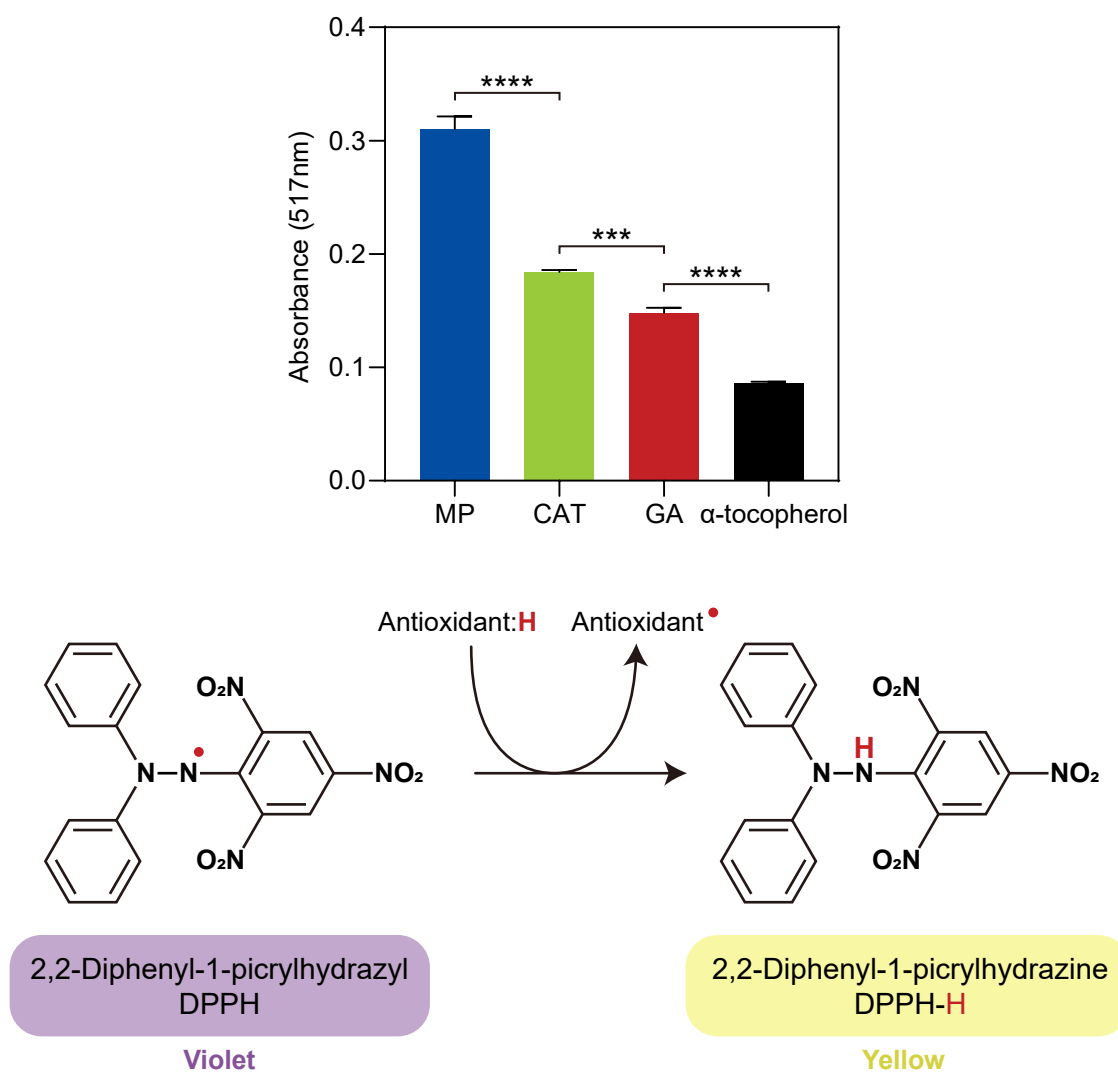


**Figure 6.** Analysis of the radical scavenging rate of CHI-MP, CHI-CAT, and CHI-GA by DPPH assay.  $\alpha$ -tocopherol was used as a positive control.